On-Line Biophysics Textbook
Volume: Separations and Hydrodynamics

Todd M. Schuster, editor

Chapter 1
Survey of Biomolecular Hydrodynamics *

Victor A. Bloomfield
Department of Biochemistry, Molecular Biology, and Biophysics
University of Minnesota
1479 Gortner Avenue
Saint Paul, Minnesota 55108
email: victor@tc.umn.edu

September 9, 2000

1 Introduction

This chapter surveys modern methods for measuring the hydrodynamic properties of biological macromolecules and for calculating the hydrodynamic properties of useful models for biomolecules. Hydrodynamic properties are quantities like sedimentation and diffusion coefficient, rotational relaxation time, intrinsic viscosity, and viscoelastic relaxation time. They enable one to determine how rapidly molecules translate and rotate in solution, and how they influence the steady-state and time-dependent viscosity of solutions. These measured properties, in turn, when interpreted in terms of suitable models, give us information about the molecular weight, size, hydration, shape, flexibility, conformation, and degree of association of biological macromolecules.

Like so much of science, hydrodynamics has a long history, but has been dramatically changed by recent advances in experiment, theory, and computation. Classic textbooks tell of the experimental work of Fick in 1855 on diffusion [1], Svedberg in the 1920s on sedimentation [2], and Poiseuille in 1846 on viscosity [3]. Theories for simple shapes such as spheres and ellipsoids were worked out by Stokes (1847) [4], Einstein (1906) [5, 6], and Perrin (1936) [7, 8]. However, recent experimental developments such as dynamic laser light scattering, nanosecond fluorescence depolarization measurements, fluorescence recovery after photobleaching, fluorescence correlation spectroscopy, pulsed field gradient NMR, and improved analytical ultracentrifuge design have made measurements of hydrodynamic properties more convenient, precise, and refined. At the same time, development of new theoretical and computational tools have enabled calculation of the properties of complex, realistic molecular models.

In this chapter we present these new techniques, along with the older but still useful ones, in a way that we hope is suitable for an audience of students and researchers in biophysics in biochemistry. We forego the heavier experimental and mathematical details and focus on physical principles, results, and applications. We also provide links to Web-based resources and computer programs that can be used to calculate hydrodynamic properties of atomic-level structures.

2 Frictional coefficients

When a particle moves in a fluid, either under the influence of an applied force or torque, or due to Brownian motion, it experiences frictional resistance. The proportionality between particle velocity and frictional resistance is the *frictional coefficient*.

The translational frictional coefficient $f_{\mathrm{t}}$is the proportionality constant between the velocity w̆ith which a particle is moving, and the frictional force $\mathbf{F}_{\mathrm{f}}$ which resists that motion:

$$\mathbf{F}_{\mathrm{f}} = -f_{\mathrm{t}}\mathbf{v}, \tag{1}$$

where the minus sign arises because the frictional force opposes the particle motion. The motion is produced by an applied force (e.g. centrifugation or electrophoresis) or by a concentration gradient, as in diffusion.

Likewise, the rotational frictional coefficient f_{r} is the constant of proportionality between the angular velocity $\boldsymbol{\omega}$ of the molecule, and the frictional torque $\mathbf{T}_{\mathrm{r}}$ resisting rotation:

$$\mathbf{T}_{\mathrm{r}} = -f_{\mathrm{r}}\boldsymbol{\omega}, \tag{2}$$

where the rotation may be produced by an applied electric or hydrodynamic flow field, or by diffusion of molecular axes.

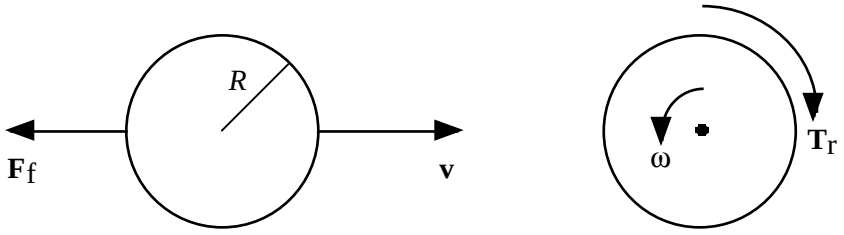

Figure 1: Frictional force and torque exerted on a translating and rotating body

2.1 Viscosity of water

All frictional coefficients depend on the viscosity of the medium in which the particles are immersed. The viscosity η is defined as the force per unit area needed to maintain unit velocity gradient between two parallel surfaces moving relative to one another in the fluid. The cgs units of η are therefore dyne-sec/cm^2, or *poise* in honor of Poiseuille who investigated the fundamental laws of viscous flow in tubes [3].

Most biopolymer experiments are conducted in water or dilute aqueous buffers. The viscosity of water is a strongly decreasing function of temperature. Hydrodynamic results are commonly

adjusted to 20°C, at which temperature the viscosity of water is 0.01002 poise, or 1.002 centipoise (cp). Values of η for water at other temperatures are tabulated in the *CRC Handbook of Chemistry and Physics* and are closely approximated by the equations

$$\log_{10}\eta = \frac{1301}{998.333 + 8.1855(t-20) + 0.00585(t-20)^2} - 3.30233 \tag{3}$$

in the range $0 \le t \le 20$°C, and

$$\log_{10}\frac{\eta}{\eta_{20}} = \frac{1.3272(20-t) - 0.001053(t-20)^2}{t+105} \tag{4}$$

in the range $20 \le t \le 100$°C, where t is the Celsius temperature.

2.2 Spheres

We will discuss in the following sections the experiments by which these frictional coefficients are measured, but it will be helpful now to have a sense of how they depend on molecular size and shape for the simplest shape, a sphere, and for other model shapes. A sphere has radius R and volume $V = (4/3)\pi R^3$. It has translational and rotational frictional coefficients

$$f_{\mathrm{t}} = 6\pi\eta R \tag{5}$$

and

$$f_{\mathrm{r}} = 8\pi\eta R^3, \tag{6}$$

Eq. 5 is known as Stokes' law, and the hydrodynamic radius R is often called the Stokes radius. Note that translational friction varies only as the first power of the molecular size, and therefore is much less sensitive to molecular dimensions than is rotational friction, which varies as R^3 or molecular volume.

2.3 Ellipsoids of revolution and cylinders

Other rigid models of macromolecules, being nonspherical, have more complex properties than spheres. The ellipsoid of revolution model is widely used because its properties can be calculated exactly [7, 8]. This is the generalization of a sphere, obtained by rotating an ellipsoid about one of its axes. The axis about which rotation occurs is called the symmetry axis, and its half-length (analogous to the radius of a sphere) is a. The half-lengths of the two other axes are equal to b. The axial ratio $a/b = p$ and the volume $V = (4/3)\pi ab^2$, an obvious generalization of the result for a sphere. Oblate ellipsoids are pancake-shaped, with $p < 1$. Prolate ellipsoids of revolution are football-shaped, with $p > 1$. They are often used as models for cylindrical rods, giving reasonably accurate results if length and volume of the two objects are equated ($2a = L, b_{\mathrm{ell}} = \sqrt{3/2}b_{\mathrm{cyl}}$). However, since cylinders do not have gradually narrowing ends, their frictional resistance, especially to rotational motion, is somewhat different from that of ellipsoids. Therefore, numerically accurate equations for cylinders have been obtained.

Translational and rotational friction coefficients for ellipsoids and cylinders are listed in Table 1. They are expressed as ratios relative to the frictional coefficients of spheres of the same volume. That is,

$$F_{\mathrm{t}} = f_{\mathrm{t}}/6\pi\eta R_{\mathrm{e}} \tag{7}$$

and

$$F_{\rm r} = f_{\rm t}/8\pi\eta R_{\rm e}^3. \tag{8}$$

The equivalent radii $R_{\rm e}$ of the spheres of equal volume are given in the first row of Table 1. For ellipsoids, $q = 1/p$; for cylinders, $p = L/2b$ where $2b$ is the diameter.

In translation, the frictional coefficients are different for movement with the long axes parallel or perpendicular to the direction of motion. However, since what is almost invariably measured is the average over all orientations, only the average is given for $F_{\rm t}$. In rotation, $F_{\rm r}(i)$ is the frictional coefficient for rotation around the ith axis (i = a or b).

Table 1: Translational and rotational frictional coefficients of ellipsoids and cylindrical rods relative to spheres of the same volume [7–11]

	Prolate ellipsoid	Oblate ellipsoid	Cylinder
$R_{\rm e}$	$(ab^2)^{1/3}$	$(ab^2)^{1/3}$	$(3/2p^2)^{1/3}(L/2)$
$F_{\rm t}$	$\frac{\sqrt{1-q^2}}{q^{2/3}\ln\frac{1+\sqrt{1-q^2}}{q}}$	$\frac{\sqrt{q^2-1}}{q^{2/3}\arctan\sqrt{q^2-1}}$	$\frac{(2p^2/3)^{1/3}}{\ln p+\gamma}, \gamma = 0.312 + \frac{0.565}{p} + \frac{0.100}{p^2}$
$F_{\rm r}(a)$	$\frac{4(1-q^2)}{3(2-2q^{4/3}/F_{\rm t}}$	$\frac{4(1-q^2)}{3(2-2q^{4/3}/F_{\rm t}}$	$0.64\left(1 + \frac{0.677}{p} - \frac{0.183}{p^2}\right)$
$F_{\rm r}(b)$	$\frac{4(1-q^4)}{3q^2\left[2q^{-2/3}(2-q^2)/F_{\rm t}-2\right]}$	$\frac{4(1-q^4)}{3q^2\left[2q^{-2/3}(2-q^2)/F_{\rm t}-2\right]}$	$\frac{2p^2}{9(\ln p+\delta}, \delta = -0.662 + \frac{0.917}{p} - \frac{0.050}{p^2}$

2.4 Random coils

A random coil has on average a spherical domain, so it is not surprising that it behaves hydrodynamically like a sphere with effective hydrodynamic radius closely related to its radius of gyration [12]. For a random coil with N bonds of length b, that is not swollen by excluded volume,

$$f_{\rm t} = 6\pi\eta\frac{3\sqrt{\pi}}{8}\left(\frac{b^2N}{6}\right) = 6\pi\eta \times 0.665 < R_g^2 >^{1/2}, \tag{9}$$

which shows that the effective hydrodynamic radius is about 2/3 of the radius of gyration $< R_g^2 >^{1/2}$. A similar relation holds for coils with excluded volume, but the numerical factor varies slowly with the excluded volume. Because of its flexibility, a random coil does not undergo a defined (rigid) rotational motion. The equivalent of a rotational relaxation time is the relaxation time τ_1 for the longest normal mode of internal motion of the coil.

2.5 Oligomeric arrays of spheres

Many proteins are effectively modeled as compact arrays of spheres. A tabulation of translational and rotational friction coefficients for various geometries is given in Table 2.

Table 2: Translational and rotational friction coefficients for arrays of n identical spheres in the indicated geometries, relative to $f_{\rm t}$and $f_{\rm r}$for the spherical monomer. 33 corresponds to rotation around the axis of highest symmetry, and 11 is for either axis perpendicular to it. [13]

n	Geometry	$F_{\rm t}$	$F_{\rm r}(11)$	$F_{\rm r}(33)$
1	Sphere	1.00	1.00	1.00
2	Dimer	1.38	3.79	1.77
3	Triangle	1.61	4.24	5.71
3	Linear	1.71	9.26	2.52
4	Square	1.82	6.29	8.40
4	Tetrahedron	1.77	6.06	6.06
4	Linear	2.00	17.86	3.27
5	Pentagon	2.04	9.01	11.90
5	Bipyramid	1.92	8.47	6.41
6	Hexagon	2.25	12.35	16.39
6	Octahedron	2.02	8.70	8.70
6	Trigonal prism	2.07	10.00	9.17
8	Cube	2.31	13.33	13.33

3 Experimental determination of hydrodynamic properties

3.1 Sedimentation coefficient

Of the various hydrodynamic techniques, the most widely used is sedimentation. Another term is centrifugation; and if the centrifuge operates at high speeds, ultracentrifugation [14]. We distinguish two types of sedimentation experiments: those in which the velocity of molecular motion is measured, and those in which the centrifuge runs until equilibrium is reached and one measures the unchanging concentration distribution. In this chapter we consider only sedimentation velocity, since it depends on the translational frictional coefficient.

In a sedimentation velocity experiment, one measures the velocity of the macromolecular solute, dissolved in solvent, in response to a centrifugal field. It is conventional in a multicomponent system to denote water as component 1, polymer solute as component 2, and other small molecular solvent components (salts, buffer, etc.) as components 3,... Consider a particle of mass m, spun with angular velocity ω at a distance r from the axis of rotation. The molecular weight of the polymer is M_2, so $m = M_2/N_A$, where N_A is Avogadro's number. If the specific volume (more rigorously, the partial specific volume) of the polymer is $\overline{v}_2$ cc/g, and the density of the solvent is ρ g/cc, each polymer molecule displaces a mass of solvent $m\overline{v}_2\rho$, so its effective buoyant mass is $M_2(1-\overline{v}_2\rho)/N_A$. The angular acceleration is $\omega^2 r$ (sometimes expressed a a multiple of g, the gravitational acceleration, equal to 980 cm/sec^2), so the centrifugal force on the particle is

$$F_{cent} = \frac{M_2}{N_A}(1-\overline{v}_2\rho)\omega^2 r. \tag{10}$$

This produces a velocity $v = dr/dt$, which is resisted by a frictional force

$$F_{fr} = -f_{\mathrm{t}} v = -f_{\mathrm{t}} \frac{dr}{dt}. \tag{11}$$

In the steady state, the sum of these forces is zero, so one can define the sedimentation coefficient S as the velocity per unit acceleration:

$$S = \frac{dr/dt}{\omega^2 r} = \frac{M_2(1 - \overline{v}_2\rho)}{N_A f_{\mathrm{t}}}. \tag{12}$$

The first of these equalities allows determination of S in terms of measurable quantities. The second enables determination, from S and the buoyancy factor, of the quotient of molecular quantities M_2/f_{t}.

The units of S are seconds (s). Generally values of S are in the range 10^{-13} to 10^{-10} s. To eliminate these small numbers, a sedimentation coefficient of 10^{-13} s is given the value of 1 Svedberg (S), after the inventor of the ultracentrifuge. The proper unit of angular velocity (ω) is rad/s, but centrifuge speeds are most commonly stated in revolutions per minute, rpm. The conversion factor is 1 rpm = $60/2\pi$ rad/s. When doing calculations, it is important to work in consistent units.

The sedimentation coefficient is determined experimentally by measuring the position, as a function of time, of the band of solute material initially layered on top of the buffer solution, or of the midpoint of the boundary formed by redistribution of the components of the initially uniform solution in the centrifugal field. Rearrangement of the first equality in eq. 12 leads to

$$\frac{dr_m}{r_m} = S\omega^2 dt \tag{13}$$

which when integrated yields

$$\ln(r_m/r_0) = S\omega^2 t, \tag{14}$$

where r_m is to be interpreted as the midpoint of band or boundary at time t, and r_o is the starting position at $t = 0$. Thus S is obtained from the slope of a plot of $\ln r_m$ vs t, divided by ω^2.

Various means are available to measure concentration distributions in sedimentation. In the modern generation of analytical ultracentrifuges, the concentration across the cell is monitored optically during the course of the run. For nucleic acids, which absorb light strongly at 260 nm, measurement of A_{260} as a function of r allows determination of the concentration distribution at quite low concentrations. For proteins, measurement around 280 nm or in the absorption band of some chromophore also allows sensitive detection. In older instruments, and even today for some purposes, refractive index measurements using schlieren or Rayleigh interference fringe techniques were employed. The concentration distribution in a preparative ultracentrifuge can be determined after a run is complete, by withdrawing and measuring solution from successive layers in the centrifuge tube. In this case, if the polymer has been radioactively labelled, or if it has some enzymatic or biological activity, very low concentrations can be detected.

There are numerous details, inappropriate for discussion here, that are important to the successful execution and interpretation of sedimentation experiments. They concern matters such as diffusional broadening, concentration dependence, and interaction of charged molecules. These are treated in monographs, manufacturer's literature, and Web sites.

3.2 Translational diffusion coefficient

Molecules in solution undergo brownian motion under thermal bombardment from their surroundings, which causes them to move even when not subject to an external force. This thermal motion, called diffusion, is random in magnitude and direction, but can be measured by the techniques described below. Diffusion is also observed when a concentration gradient is set up in solution or when a barrier between solutions at two different concentrations is removed. The tendency toward equalization of concentrations is attributable at the macroscopic level to a gradient of concentration or chemical potential; but at the molecular level it can also be understood as the random motion of molecules, with more molecules in the concentrated region of solution available to move randomly into the more dilute region.

The rate of brownian motion or evening-out of concentration gradients is proportional to the translational diffusion coefficient D_t, which in turn is inversely proportional to f_t. In this section we summarize the basic laws characterizing translational diffusion, and describe some of the most important modern techniques whereby D_t can be measured.

We note that molecules also undergo *rotational* brownian motion. This will be discussed later.

3.2.1 Fick's laws of diffusion

At the macroscopic level, two basic equations describe the change of concentration as a function of position and time under the influence of translational diffusion. The first is Fick's first law, which states that the flux $\boldsymbol{J}$ of matter across an imaginary surface per unit area and per unit time is proportional to the concentration gradient and the diffusion coefficient:

$$J(x,t) = -D_\mathrm{t}\left[\frac{\partial c(x,t)}{\partial x}\right]_t, \tag{15}$$

where we have written the one-dimensional equation for simplicity. Note that this equation states that a positive flux occurs from high to low concentration.

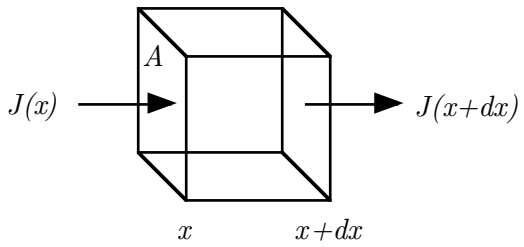

Figure 2: Fluxes into and out of an infinitesimal volume element.

If we consider an infinitesimal volume element dV in solution of cross-sectional area A and thickness dx located at x, conservation of mass requires that the difference between the flow of matter into the element and the flow out must equal the amount accumulated within the element:

$$[J(x,t) - J(x+dx,t)]\,A = \left[\frac{\partial J(x,t)}{\partial x}\right]_t A dx = \left[\frac{\partial c(x,t)}{\partial t}\right]_x dV, \tag{16}$$

where the middle equality comes from expanding $J(x + dx)$ in a Taylor's series about x. Since $dV = Adx$, we may substitute eq. (15) into eq. (16) to obtain Fick's second law:

$$\left[\frac{\partial c(x,t)}{\partial t}\right]_x = D_t \left[\frac{\partial^2 c(x,t)}{\partial x^2}\right]_t, \tag{17}$$

where we have assumed that D_t is independent of c, and hence independent of x.

The solution of eq. (17) for the initial condition in which there is a very narrow (delta function) spike of material c_0 at $x = x_0$, and zero concentration elsewhere, is

$$c(x,t) = \frac{c_0}{\sqrt{4\pi D_t t}} e^{-\frac{(x-x_0)^2}{4D_t t}}. \tag{18}$$

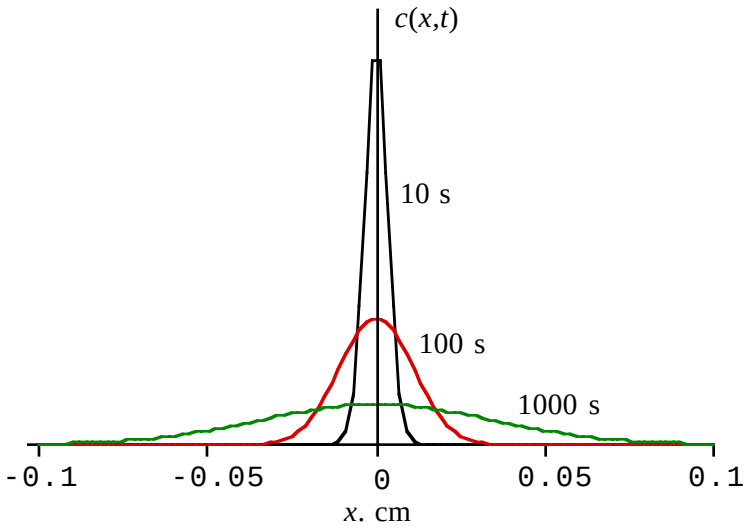

Figure 3: Concentration profile from an initial spike at $x = 0$ after 10, 100, and 1000 s, for a protein with typical diffusion coefficient $D = 6 \times 10^{-7}$ cm^2/s.

3.2.2 Frictional resistance and brownian motion

Given its physical meaning, it seems reasonable that D_t should increase as the thermal energy of the solution increases, and decrease with the frictional resistance to translational motion. In fact, as Einstein showed in 1906, the relation is

$$D_t = \frac{k_B T}{f_t}. \tag{19}$$

An important physical consequence of Fick's second law relates the mean-square distance diffused in time t to the diffusion coefficient:

$$< x^2 >= 2D_t t. \tag{20}$$

This equation can be derived from the solution to Fick's second law for an initial sharp spike of concentration located at $x_0 = 0$ (see eq. (18)), or by probabilistic considerations of molecules in regions of different concentrations moving randomly along the x-axis. The two- and three-dimensional analogs of eq. (20) are

$$< \rho^2 >= 4D_{\mathrm{t}}t \tag{21}$$

and

$$< r^2 >= 6D_{\mathrm{t}}t, \tag{22}$$

respectively. The dependence of average distance traveled on the *square root* of the time means that diffusion is an efficient way of traversing short distances, on the order of a membrane thickness or the interior of a small cell, but is very inefficient for traversing longer distances.

3.2.3 Diffusion across a porous barrier

A classical method of determining D_{t}, particularly useful for small molecules such as drugs, is to place different concentrations c_1 and c_2 on opposite sides of a porous barrier of thickness Δx and area A. The molecules can either be radioactively labeled or have some optical property that enables measurement of their concentrations as a function of time. The solutions on the two sides of the barrier are stirred to disrupt stagnant boundary layers and make concentrations uniform on each side. The amount of material Δm that flows across the barrier in unit time is given by Fick's first law, eq. (15) in the finite difference form

$$\Delta m = JA = -AD_{\mathrm{t}}\frac{\Delta c}{\Delta x} \tag{23}$$

where $\Delta c = c_2 - c_1$. Since A and Δx are generally not measurable accurately, the apparatus is calibrated with a compound of known D_{t} to obtain $A/\Delta x$. Then measurement of Δm for the unknown enables calculation of its diffusion coefficient.

3.2.4 Broadening of sedimentation boundaries

In a sedimentation velocity experiment, the boundary will broaden with time due to diffusion as it moves down the cell. Exact analysis of the broadening is complicated by the radial sector shape of the cell and by the concentration dependence of D_{t} (an effect not treated in this chapter). However, to a reasonable approximation the width of the boundary (approximately the standard deviation of a Gaussian profile) will be given by eq. (20), $< x^2 >= 2D_{\mathrm{t}}t$.

3.2.5 Dynamic laser light scattering

Much of the modern determination of diffusion coefficients of macromolecules is done by dynamic laser light scattering (also called quasielastic light scattering or photon correlation spectroscopy) [15, 16]. As molecules diffuse under the influence of Brownian motion, the electric field $E_s(t)$ and intensity $I_s(t) = |E_s(t)|^2$ scattered from them fluctuate with time. The time variation thus gives information on particle motions.

There are three types of fluctuations to be considered in dynamic light scattering experiments.

1. Occupation number fluctuations are due to fluctuations in the number of particles N in the scattering volume. From Poisson statistics, we know that these fluctuations are inversely proportional to $\sqrt{N}$. To have fluctuations at the 1% level, N must be 10^4 or less in a scattering volume typically 1 mm on a side. This is a very low concentration, hence only very strong scatterers, such as whole cells, will produce measurable occupation number fluctuations. These are not generally important for macromolecules. Further, since particles must diffuse a distance of about 1 mm to enter or exit the scattering volume, occupation number fluctuations are slow, typically on the order of seconds.

2. Amplitude fluctuations result from rotation and internal motions of molecules. In order to be observable, these motions must have a characteristic length that is not too small compared to the wavelength λ. Such internal fluctuations are readily observed, if not always readily interpreted, in the dynamic scattering from large DNA molecules and protein polymers.

3. Most important, phase fluctuations arise from translation of molecule over a distance comparable to the wavelength λ. These fluctuations are rapid and observable from molecules over a very wide range of sizes. The characteristic time scale for phase fluctuations due to translational diffusion can be estimated from eq. (20). The distance travelled to produce a measurable change in the phase of the scattered light (i.e. a change in amplitude which is a significant fraction of the peak-to-trough amplitude) is on the order of $\lambda/10$. Thus, eq. (20) yields $t \approx (\lambda/10)^2/2D_\mathrm{t}$. With λ_0 about 5000 Å in vacuo, corresponding to about 3.8×10^{-5} cm in aqueous solution with refractive index $n = 1.33$, and a typical D_t of 10^{-7} cm^2/s, this gives $t \approx 7 \times 10^{-5}$ seconds. The microsecond to millisecond range for dynamic light scattering fluctuations is observed for most biological macromolecules. Thus dynamic light scattering can be used for very rapid measurement of D_t.

The dynamic light scattering equations are derived in a more complete and systematic fashion in numerous sources (e.g. Berne & Pecora, 1976; Bloomfield & Lim, 1978; Schmitz, 1990; Chu, 1991). The important result is that the autocorrelation function $g_2(t)$ of the photocurrent resulting from the scattered light is

$$g_2(t) = 1 + \beta e^{-2q^2 D_\mathrm{t} t} \tag{24}$$

where β is an instrumental constant and q is the scattering vector, $(4\pi n/\lambda_0)\sin(\theta/2)$ where θ is the scattering angle. This equation showns that $-2q^2 D_\mathrm{t}$ is the slope of a semilogarithmic plot of $g_2(t) - 1$ vs t. Since q^2 is known, D_t can be determined.

3.2.6 Fluorescence photobleaching recovery

A useful method for determining 2-dimensional diffusion in cell membranes or in concentrated solutions is fluorescence photobleaching recovery (FPR), sometimes called fluorescence recovery after photobleaching (FRAP). The simplest realization of the method, which is all we will discuss here, is to briefly illuminate a cross-section of fluorescent molecules with a narrow, intense laser beam under a microscope. The fluorophore may be a protein such as green fluorescent protein, GFP, perhaps in a genetically engineered construct with another protein of interest. Or it may be a fluorescent label bound to a protein, nucleic acid, or lipid. If the laser wavelength is in the absorption band of the fluorophore, some of the molecules exposed to the beam will be "bleached" (i.e., their fluorescence will be permanently quenched by a photochemical reaction). Then if the

fluorescence intensity F from the bleached region is monitored by a probe or reading laser beam (usually the same as the bleaching beam, but greatly attenuated so as not to cause additional photobleaching), it will initially be found to be less than F before the bleach. However, as time proceeds, molecules from adjacent regions will diffuse into the bleached region, increasing F until it eventually recovers its initial value. (If the fluorophores are constrained by attachment to a cytoskeletal or membrane network, full recovery may not be achieved. This makes FPR a useful indicator of such attachment in cell biology research.)

In the most common case the laser beam has a Gaussian profile of radius w (the radius at which the intensity has decreased to e^{-2} of its central maximum intensity). Then the time-dependence of the fractional recovery of fluorescence is determined by the function

$$\theta(t) = \frac{1}{1 + t/\tau_D}, \tag{25}$$

where the characteristic recovery time τ_D is (see eq. (21))

$$\tau_D = \frac{w^2}{4D_{\mathrm{t}}}. \tag{26}$$

3.2.7 Pulsed field gradient NMR

With the increasing availability of high-field NMR spectrometers, the use of pulsed field gradient NMR to measure translational diffusion of both small molecules and macromolecules has become common. The basic idea is that if a magnetic field gradient G is applied to the sample in the NMR probe, in the same direction as the dominant magnetic field H_0, the magnetization M will change as the molecules diffuse to different regions of the gradient.

In the most common realization of the experiment [17], Fourier transform pulse techniques are used. A four-step sequence is used:

1. 90° pulse;
2. linear field gradient pulse of duration δ;
3. 180° pulse after time τ;
4. second, identical, field gradient pulse at time Δ after the first.

The resulting magnetization, relative to that with no field gradient, is then

$$\frac{M(G)}{M(0)} = \exp\left[-\gamma^2 G^2 \delta^2 (\Delta - \delta/3) D_{\mathrm{t}}\right], \tag{27}$$

where γ is the magnetogyric ratio.

3.3 Rotation

We see by comparing eqs. (5) and (6) that rotational frictional resistance varies as R^3 rather than R; that is, rotation is much more sensitive to small changes in molecular size. This makes it a very useful probe of small conformational changes. Thanks largely to advances in lasers and electronics, which can measure processes on the nanosecond to microsecond time scale, methods that measure

the rotational motion of proteins and nucleic acids have become important in characterizing their structures in solution. Detection of rotational motion generally depends on differences in optical properties of biomolecules along their principal molecular axes.

3.3.1 Rotational diffusion coefficients and relaxation times

For simplicity we shall assume that the orientation of the molecule of interest can be described by a single angle θ. Under the influence of randomizing Brownian motion, a function $f(\theta, t)$ of the orientation of a molecular axis will exponentially decay, or relax, with a characteristic time constant:

$$f(\theta, t) = f(\theta, 0)e^{-t/\tau_r}. \tag{28}$$

This rotational relaxation time is denoted τ_r, and is inversely proportional to the rotational diffusion coefficient D_r, which has units of reciprocal seconds, s^{-1}. The relation between D_r and f_r the rotational frictional coefficient, is the same for rotation as for translation:

$$D_\mathrm{r} = \frac{k_\mathrm{B}T}{f_\mathrm{r}}. \tag{29}$$

There are two commonly defined rotational relaxation times, depending on the experiment being performed. The first, $\tau_r^{(1)}$, is obtained by experiments, such as dielectric relaxation, that directly measure the orientation, $f^{(1)}(\theta) = \cos(\theta)$, of the molecular axis with respect to an external field.

The second type of relaxation time, $\tau_r^{(2)}$, is obtained in experiments (more common in contemporary practice) such as fluorescence anisotropy, electric dichroism, and NMR relaxation, that measure the orientation function $f^{(2)}(\theta) = \frac{1}{2}(3\cos^2(\theta) - 1)$. One can show that the relaxation time of axis a by rotational diffusion about axes b and c is $1/\tau_a^{(1)} = D_{r,b} + D_{r,c}$. For a sphere, with three equivalent axes,

$$\tau_r^{(1)} = \frac{1}{2D_\mathrm{r}} = \frac{f_\mathrm{r}}{2k_\mathrm{B}T}. \tag{30}$$

Also for a sphere,

$$\tau_r^{(2)} = \frac{1}{6D_\mathrm{r}} = \frac{f_\mathrm{r}}{6k_\mathrm{B}T}. \tag{31}$$

Combining this with eq. (6) and the volume $V = \frac{4}{3}\pi R^3$, we get the elegantly simple result

$$\tau_r^{(2)} = \frac{\eta V}{k_\mathrm{B}T} \tag{32}$$

Since this result was first obtained by Debye, it is sometimes known as the Debye relaxation time. Results for molecular models of other shapes, such as ellipsoids of revolution and rigid rods, are given later in this chapter. In all cases it is found that τ_r varies roughly according to V or R^3, where R is some characteristic linear dimension.

3.3.2 Photoselection: Fluorescence and Triplet State Anisotropy Decay

Techniques that measure rotational motion can be divided into two basic classes: those that orient molecules by application of an external field, and those that use polarized light to select molecules

that are already oriented along the polarization direction. The most widely used of the photoselection techniques is fluorescence anisotropy decay, also known as fluorescence depolarization, which probes motions in the nanosecond time regime. A thorough discussion is given by Cantor and Schimmel (1980, pp. 454-465).

To understand photoselection techniques requires the concept of the electronic transition dipole moment $\boldsymbol{\mu}_a$, which can be qualitatively understood as the dipole produced by the electronic motion under the influence of the electric field of the incident light. Fluorescence involves first the absorption and then the emission of light. If the exciting light is vertically plane-polarized with electric field $\mathbf{E}$ along the z-axis, then only those molecules with a component of their absorption transition dipole moment $\boldsymbol{\mu}_a$ in the same direction as $\mathbf{E}$ will be able to absorb. The amplitude of $\mathbf{E}$ along $\boldsymbol{\mu}_a$ is $\mathbf{E} \cdot \boldsymbol{\mu}_a = E\mu_a \cos\theta$, and the intensity of absorption, proportional to the square of the amplitude, varies as $\cos^2\theta$. Thus those molecules with $\cos\theta$ near 1 will be preferentially excited.

Assume initially that the system is rigid, so that the molecule does not rotate between excitation and emission, because it is very large or because the solution is effectively frozen. The fluorescence emission is polarized along the direction of the emission transition dipole moment $\boldsymbol{\mu}_e$. In the simplest and most common case, $\boldsymbol{\mu}_a$ and $\boldsymbol{\mu}_e$ are coincident. If the amplitude of the fluorescence electric field is F, then the component of the intensity of a single emission event in the direction of the excitation direction will be $(F\mu_e)^2 \cos^2\theta$. This is multiplied by the probability that the molecule was excited in the first place, $\cos^2\theta$. Thus the total intensity of fluorescence along the excitation direction, $F_\parallel$, will be proportional to $< \cos^4\theta >$ where the angular brackets denote an average over the whole population of fluorescent molecules. Likewise, the probability of emission perpendicular to the excitation direction, $F_\perp$, will be proportional to $< \cos^2\theta \sin^2\theta cos^2\phi >$ where ϕ is the azimuthal angle and $\sin\theta\cos\phi$ is the projection of μ_e on the x-axis. The values of these averages are $F_\parallel = 1/5$ and $F_\perp = 1/15$.

Experimentally, one defines the fluorescence anisotropy as the difference between fluorescence intensity emitted parallel and perpendicular to the exciting field, normalized by the total emitted intensity (there are one parallel and two perpendicular directions of emission):

$$A = \frac{F_\parallel - F_\perp}{F_\parallel + 2F_\perp}. \tag{33}$$

The maximum possible value of this quantity, assuming that the molecules are randomly oriented at excitation, have not rotated at all during the interval between excitation and fluorescence, and that the absorption and emission transition dipoles are coincident, is calculated as $A_0 = 2/5$ from the values of $F_\parallel$ and $F_\perp$ for a rigid system. In the more general case, $bfmu_e$ and $\boldsymbol{\mu}_a$ may not be the same, if intersystem crossing has occurred during excitation and vibrational relaxation. If the angle between $\boldsymbol{\mu}_a$ and $\boldsymbol{\mu}_e$ is ξ, the value of the anisotropy for a rigid system is calculated to be $A_0 = (3\cos^2\xi - 1)/5$.

Now consider the case in which the molecules rotate in the time between excitation and emission. This period is typically a few picoseconds to a few nanoseconds, during which the electronic excitation energy is redistributed within the molecule (primarily by transfer into vibrational modes) and/or transferred to surrounding solvent, and then emitted as a red-shifted photon as the molecule drops from excited singlet S_1 to ground state singlet S_0. The orientations of the molecules change as they rotate, so the fluorescence anisotropy and polarization will change. In the limiting case that rotation is very fast compared to emission, all initial orientation information will be lost, so A will decay to zero.

In the more general (and more useful) case, rotational relaxation time τ_r and fluorescence lifetime τ_F will be comparable. Then the parallel and perpendicular components of the emission will decay with time for two reasons: the fraction of molecules in the excited state decays according to $\exp(-t/\tau_F)$, and the orientation according to $\exp(-t/\tau_r^{(2)})$. The result (Cantor and Schimmel, p. 461) is

$$A(t) = (2/5)\exp(-t/\tau_r^{(2)})[(3\cos^2\xi - 1)/2]. \tag{34}$$

Thus the time-dependence of the anisotropy can be used to determine $\tau_r^{(2)}$, and thereby provide information on molecular size and shape.

If the experiments are done in the steady-state rather than in a time-resolved manner, then one must average separately over the time dependence of components $F_\parallel$ and $F_\perp$ before computing the steady-state anisotropy $< A >$. The result is conveniently written in reciprocal form as

$$< A >^{-1} = A_0^{-1}\left(1 + \frac{\tau_F}{\tau_r^{(2)}}\right) = A_0^{-1}\left(1 + \tau_F\frac{k_\mathrm{B}T}{\eta V}\right) \tag{35}$$

Another commonly used measure of anisotropy, particularly in the older literature, is the polarization P, defined as

$$P = \frac{F_\parallel - F_\perp}{F_\parallel + F_\perp}. \tag{36}$$

which has maximum value $P_0 = 1/2$ for a rigid system. Algebraic rearrangement shows that

$$\left(\frac{1}{P} - \frac{1}{3}\right)^{-1} = \frac{3}{2}A, \tag{37}$$

so the equation for the steady-state polarization is

$$\left(\frac{1}{P} - \frac{1}{3}\right) = \left(\frac{1}{P_0} - \frac{1}{3}\right)\left(1 + \frac{\tau_F}{\tau_r^{(2)}}\right) = \left(\frac{1}{P_0} - \frac{1}{3}\right)\left(1 + \tau_F\frac{k_\mathrm{B}T}{\eta V}\right) \tag{38}$$

These are known as the Perrin equations (Perrin, 1934). Thus the molecular volume V can be obtained, if τ_F is known by independent measurement, by measuring $1/ < A >$ or $1/ < P >$ as a function of T/η. In these experiments, the viscosity is generally varied by changing the temperature (for water, η changes by 2% for each centigrade degree) or by adding an inert compound such as sucrose or glycerol to the solution.

The equations in this section are strictly valid only for rigid, spherical molecules. If the molecule is substantially nonspherical, the expressions become significantly more complicated, owing to the contributions from rotations about the nonequivalent axes. In the limit, as many as five relaxation times may enter into the decay of the anisotropy, though it is rare that more than two can be resolved experimentally. Another complexity arises if the chromophore has substantial independent mobility within the macromolecule. The measured rotational relaxation time will then be much shorter than that corresponding to the macromolecular dimensions. On the other hand, approximate equality of measured and calculated relaxation times indicates that the chromophore moves rigidly with the macromolecule.

3.4 Intrinsic viscosity

The viscosity of a fluid reflects its resistance to flow under an applied force. Viscosity is useful in the study of biopolymers because the addition of large molecules to a solvent increases its viscosity; the increase depends on the concentration, size, and structure of the polymer. Motion in one layer of a fluid causes motion in adjoining layers. To move layers with different relative velocities requires a force: the more viscous, the more force. The quantitative description of this relation was first enunciated by Newton. Suppose two parallel planes in the fluid each have area A, and are separated by distance h. If the upper plane moves with velocity v relative to the lower, then the shearing force F needed to maintain this velocity differential is

$$F = \eta \frac{Av}{h}. \tag{39}$$

The coefficient of proportionality, η, is called the viscosity. It can be seen to have units of dyne/cm^2-s, or poise, in honor of the 19th C French physician Poiseuille, who investigated the flow of liquids in tubes. Water at 20°C has a viscosity of 0.01 poise, or 1 centipoise.

Two factors influence F: the strength of the force between layers (greater in molasses than in water, and in water than in air), and the linear extent of the interactions. A cell extract is so viscous because the entangled network of macromolecules extends from one side of the container to the other, and the motion of one part of the fluid, e.g. in pouring or stirring, is retarded by interactions with molecules far away (in regions with different velocities) mediated by intervening molecular interactions. This suggests that viscosity will decrease as polymer concentration decreases, since the probability of intermolecular interactions and the spans of intermolecular complexes will decrease.

This molecular picture predicts that bigger polymers, when dissolved in solution, will raise the viscosity more than smaller molecules since their molecular domain has a greater extent. This concept was made quantitative by Einstein, who showed that for spheres occupying volume fraction ϕ in dilute solution, the solution viscosity relative to solvent viscosity ho is

$$\eta = \eta_0 \left(1 + \frac{5}{2}\phi\right). \tag{40}$$

The volume fraction (cc polymer/cc solution) can be expressed as the volume occupied by one gram of hydrated polymer, v_h (cc polymer/g polymer), times the weight concentration of polymer c_2 (g polymer/cc solution). Thus eq. (40) can be rearranged to yield

$$\frac{\eta - \eta_0}{\eta_0 c_2} = \frac{5}{2} v_h. \tag{41}$$

It is customary to measure η at several concentrations and extrapolate to $c_2 = 0$. This yields the intrinsic viscosity $[\eta]$:

$$[\eta] = \lim_{c_2 \to 0} \frac{\eta - \eta_0}{\eta_0 c_2} = \frac{5}{2} v_h \tag{42}$$

for spheres. For non-spherical particles, the factor $\frac{5}{2}$ is replaced by a parameter $\nu > \frac{5}{2}$. Since intrinsic viscosity is rarely measured these days, we do not give these results, but refer the reader to the literature.

References

[1] A. Fick (1855) Ann. Physik 23: 59.

[2] Svedberg 1920s

[3] J.L.M. Poiseuille (1846) Mémoirés présentés par divers savants á l'academie royale des sciences de l'institute de France 9: 433.

[4] Stokes 1847

[5] Einstein 1906

[6] A. Einstein (1985) Investigations on the Theory of the Brownian Movement, Dover, New York.

[7] Perrin, F. (1934) Mouvement brownien d'un ellipsoide (I). Dispersion dielectrique pour des molecules ellipsoidales, J. Phys. Radium [7] 5, 497-511.

[8] Perrin, F. (1936) Mouvement brownien d'un ellipsoide (II). Rotation libre et depolarisation des fluorescences. Translation et diffusion de moleculesellipsoidales, J. Phys. Radium [7]7, 1-11.

[9] Koenig, S. (1975) Brownian motion of an ellipsoid. A correction to Perrin's results, Biopolymers 14, 2421-2423.

[10] Tirado, M.M. and J. Garca de la Torre (1979) Translational friction coefficients of rigid, symmetric top macromolecules. Application to circular cylinders, J. Chem Phys. 71: 2581-2588.

[11] Tirado, M.M. and J. Garca de la Torre (1980) Rotational diffusion of rigid, symmetric top macromolecules. Application to circular cylinders, J. Chem Phys. 73, 1986-1993.

[12] Kirkwood, J.G. and J. Riseman (1956) in Eirich, F., ed. Rheology, Vol. 1, p. 495, Academic Press, New York.

[13] García de la Torre, J. and V. A. Bloomfield. 1981. Hydrodynamic properties of complex, rigid, biological macromolecules: Theory and applications. *Q. Rev. Biophys.*. 14: 81–139.

[14] Schuster, T.M. and T.M. Laue, eds. (1994) *Modern Analytical Ultracentrifugation : Acquisition and Interpretation of Data for Biological and Synthetic Polymer Systems*, Springer-Verlag, New York.

[15] Berne, B. J. and R. Pecora. (1976). *Dynamic Light Scattering with Applications to Chemistry, Biology, and Physics*, Wiley-Interscience, New York.

[16] Santos, N.C. and M.A.R.B. Castanho (1996) Teaching Light Scattering Spectroscopy: The Dimension and Shape of Tobacco Mosaic Virus, Biophys. J. 71(3): 1641-1650. (A .pdf version is available in the *Biophysical Society On-line Textbook* at http://biosci.umn.edu/biophys/OLTB/BJ/BJ-Teach.html)

[17] T.L. James and G.G. McDonald (1973) J. Mag. Res. 11: 58.

[18] T.L. James (1975) *Nuclear Magnetic Resonance in Biochemistry: Principles and Applications*, Academic Press, New York. Chapter 5.8.